

Heavy-Metal Aromatic Rings: Cyclopentadienyl Anion Analogues Sn_5^{6-} and Pb_5^{6-} in the Zintl Phases Na_8BaPb_6 , Na_8BaSn_6 , and Na_8EuSn_6

Iliya Todorov and Slavi C. Sevov*

Department of Chemistry and Biochemistry, University of Notre Dame, Notre Dame, Indiana 46556

Received June 23, 2004

The title compounds were prepared by direct reactions of the corresponding elements at high temperature. They are isostructural with each other (monoclinic, $P2_1/m$, $Z = 2$; Na_8BaPb_6 , $a = 13.116(4)$, $b = 5.351(1)$, and $c = 16.166(5)$ Å, $\beta = 108.07(2)^\circ$; Na_8BaSn_6 , $a = 12.897(4)$, $b = 5.362(1)$, and $c = 16.826(5)$ Å, $\beta = 108.19(2)^\circ$; Na_8EuSn_6 , $a = 12.912(2)$, $b = 5.220(1)$, and $c = 15.721(2)$ Å, $\beta = 108.09(1)^\circ$) and contain isolated, flat, and aromatic pentagonal rings of Sn_5^{6-} and Pb_5^{6-} as well as isolated anions of Sn^{4-} and Pb^{4-} . According to four-probe conductivity measurements, the tin compounds, Na_8BaSn_6 and Na_8EuSn_6 , are semiconducting with band gaps of 0.11 and 0.09 eV, respectively, and are therefore electronically balanced. Magnetic measurements show that Na_8BaSn_6 is diamagnetic while Na_8EuSn_6 is paramagnetic and undergoes two transitions at low temperatures.

Introduction

Until recently, the only deltahedral clusters of group 14 (tetrels, Tt) known in neat solids (made by solid-state reaction) with the alkali metals (A) were the tetrahedral Tt_4^{4-} and the *nido*-species Tt_5^{4-} .^{1,2} They were later supplemented by the eight-member *arachno*-clusters of tin Sn_8^{6-} in $\text{K}_4\text{Li}_2\text{-Sn}_8$ and $\text{Rb}_4\text{Li}_2\text{-Sn}_8$.³ The synthesis of the later was possible only because of the use of mixture of alkali metals of very different sizes, Li and K or Li and Rb in this case. Clearly, in many cases, the approach of using cations that differ in size and/or charge leads to different tuning of the balance between packing and electronic requirements and ultimately stabilizes novel clusters or extended structures in the solid state. Another noteworthy example of the “power” of cations

with different sizes is RbLi_7Ge_8 with isolated giant clusters of Ge_{12}^{12-} with the shape of truncated tetrahedra.⁴ It should be pointed out that the role of the lithium cations in these compounds is not only to reduce the p-element and occupy little space but also to interact covalently with the anionic substructure. Thus, they cap the square faces of Sn_8^{6-} completing the cluster to a “*closo*” bicapped square antiprism of $[\text{Li}_2\text{Sn}_8]^{4-}$.³ Similarly, they cap the hexagonal faces of Ge_{12}^{12-} completing the cluster to a “*closo*” $[\text{Li}_4\text{Ge}_{12}]^{8-}$.⁴

The approach of using cations with different sizes was later extended into “doping” of alkali metal–tetrel binary systems with alkaline-earth cations (Ae). This approach led to stabilization of Sn_{12}^{12-} in $\text{Na}_{10}\text{AeSn}_{12}$ (Ae = Ca, Sr)⁵ and the largest ever tin-cluster Sn_{56}^{36-} in $\text{Na}_{204}\text{Ba}_{16}\text{Sn}_{310}$.⁶ While studying the cation-rich side of these systems, we discovered the isostructural compounds reported here, Na_8BaPb_6 (**1**), Na_8BaSn_6 (**2**), and Na_8EuSn_6 (**3**). They contain isolated flat pentagonal rings of Sn_5^{6-} and Pb_5^{6-} as well as isolated monatomic anions of Sn^{4-} and Pb^{4-} . The rings can be described as *arachno*-clusters according to Wade’s rules,⁷ but more intriguingly, they can be viewed as all-metal (and very heavy metal at that!) aromatic species according to the rules for aromaticity.

* Author to whom correspondence should be addressed. E-mail: ssevov@nd.edu.

- (1) (a) Shafer, H. *Annu. Rev. Mater. Sci.* **1985**, *15*, 1. (b) Fassler, T. F.; Hoffmann, S. Z. *Kristallogr.* **1999**, *214*, 722 and references therein.
- (2) (a) Queneau, V.; Sevov, S. C. *Angew. Chem., Int. Ed. Engl.* **1997**, *36*, 1754. (b) Queneau, V.; Todorov, E.; Sevov, S. C. *J. Am. Chem. Soc.* **1998**, *120*, 3263. (c) Queneau, V.; Sevov, S. C. *Inorg. Chem.* **1998**, *37*, 1358. (d) Todorov, E.; Sevov, S. C. *Inorg. Chem.* **1998**, *37*, 3889. (e) von Schnering, H.-G.; Baitinger, M.; Bolle, U.; Carrillo-Cabrera, W.; Curda, J.; Grin, Y.; Heinemann, F.; Llanos, L.; Peters, K.; Schmeding, A.; Somer, M. Z. *Anorg. Allg. Chem.* **1997**, *623*, 1037. (f) von Schnering, H.-G.; Somer, M.; Kaupp, M.; Carrillo-Cabrera, W.; Baitinger, M.; Schmeding, A.; Grin, Y. *Angew. Chem., Int. Ed.* **1998**, *37*, 2359.
- (3) Bobev, S.; Sevov S. C. *Angew. Chem., Int. Ed.* **2000**, *39*, 4108.

- (4) Bobev, S.; Sevov S. C. *Angew. Chem., Int. Ed.* **2001**, *40*, 1507.
- (5) Bobev, S.; Sevov S. C. *Inorg. Chem.* **2001**, *40*, 5361.
- (6) Bobev, S.; Sevov S. C. *J. Am. Chem. Soc.* **2002**, *124*, 3359.
- (7) Wade, K. *Adv. Inorg. Chem. Radiochem.* **1976**, *18*, 1.

Table 1. Selected Data Collection and Refinement Parameters for Na₈BaPb₆, Na₈BaSn₆, and Na₈EuSn₆

param	Na ₈ BaPb ₆	Na ₈ BaSn ₆	Na ₈ EuSn ₆
fw	1564.40	1033.40	1048.02
space group, <i>Z</i>	<i>P</i> 2 ₁ / <i>m</i> , 2	<i>P</i> 2 ₁ / <i>m</i> , 2	<i>P</i> 2 ₁ / <i>m</i> , 2
<i>a</i> (Å)	13.116(4)	12.897(5)	12.912(2)
<i>b</i> (Å)	5.351(1)	5.362(5)	5.220(1)
<i>c</i> (Å)	16.166(5)	15.826(3)	15.721(2)
β (deg)	108.07(2)	108.19(2)	108.09(1)
<i>V</i> (deg)	1078.7(5)	1039.8(6)	1007.4(2)
radiatn (λ , Å)	Mo K α (0.710 73)	Mo K α (0.710 73)	Mo K α (0.710 73)
temp (°C)	20	20	20
ρ_{calc} (g·cm ⁻³)	4.806	3.293	3.470
μ (cm ⁻¹)	48.471	9.066	10.566
R1/wR2, ^a <i>I</i> \geq 2 σ _{<i>I</i>} (%)	4.74/12.92	4.75/13.33	5.58/14.93
R1/wR2, ^a all data (%)	5.41/13.34	5.52/13.99	7.68/16.07

^a R1 = $[\sum||F_o| - |F_c||]/\sum|F_o|$; wR2 = $\{[\sum w[(F_o)^2 - (F_c)^2]^2]/[\sum w(F_o)^2]\}^{1/2}$; $w = [\sigma^2(F_o)^2 + (AP)^2 + BP]^{-1}$, where $P = [(F_o)^2 + 2(F_c)^2]/3$ and $A/B = 0.0849/27.0991$, $0.0856/27.9689$, and $0.079/40.4978$ for **1–3**, respectively.

Experimental Section

Synthesis. All manipulations were performed in an argon-filled glovebox (moisture level below 0.1 pm). Initially Na₈BaPb₆ was found as a minor phase of a reaction with nominal composition “Na₁₀BaPb₁₂” intended to produce the Pb analogue of Na₁₀AeSn₁₂.⁵ The other products of this reaction were NaPb and traces of Ba₃Pb₅, both identified by single-crystal and powder X-ray diffraction. After the stoichiometry of Na₈BaPb₆ was elucidated from its structure determination, all three new compounds were synthesized as single phases. The starting materials Ba (rod, Alfa 99.2%), Eu (ingot, Ames Laboratory DOE, 99.9%), Sn (rod, Alfa, 99.999%), and Pb (rod, Alfa, 99.9998%) were used as received while the surface layer of Na (ingot, Alfa, 99.9%) was removed before use. In a typical reaction the elements are mixed in a niobium ampule that is sealed by arc-welding under argon. This container is then placed in a fused-silica tube that is then evacuated and flame-sealed. The assemblies were heated at 760 °C for 1 week and were cooled to room temperature at different rates varying from 1 to 0.1 °C/min. The compounds are most likely incongruently melting since the highest yields were observed for the fastest cooling rates. Samples quenched in ice–water showed no impurities. The purity of the products was confirmed by powder X-ray diffraction on an Enraf-Nonius Guinier camera under vacuum (Cu K α radiation, $\lambda = 1.540\ 562$ Å). The samples for this analysis were well-ground powders sealed between two pieces of scotch tape to minimize exposure to air and moisture during the transfer from the glovebox to the camera. Sometimes minor quantities of lead or tin were observed, but they are most likely generated by hydrolysis and/or oxidation of the compounds during the exposure or transfer.

Structure Determination. Black barlike crystals with some metallic luster were selected from each compound and were mounted in thin-walled glass capillaries that were subsequently flame-sealed at both ends. The crystals were checked for singularity, and X-ray diffraction data sets were collected for the best ones (**1**, $0.2 \times 0.1 \times 0.1$ mm; **2**, $0.25 \times 0.04 \times 0.04$ mm, **3**, $0.2 \times 0.1 \times 0.1$) on an Enraf-Nonius CAD4 diffractometer with graphite-monochromated Mo K α radiation ($\lambda = 0.710\ 73$ Å) at room temperature (a quadrant of a sphere for each structure, ω – 2θ scans, $\theta_{\text{max}} = 25^\circ$). The raw data of **2** and **3** were each corrected for absorption with the aid of the average of 3 ψ -scans, while no appropriate reflections could be found for **1**. The structures were solved and refined on F^2 in the centrosymmetric space group *P*2₁/*m* with the aid of the SHELXTL-V5.1 software package. Direct methods provided the positions of Sn, Pb, and the heavier cations. The Na cations were later located from difference Fourier maps. Some remaining electron density was observed near two sodium

atoms, Na7 and Na8, that also had somewhat larger thermal displacement parameters. These factors suggested fractional occupancies and when freed to vary the occupancies of these two atoms deviated significantly from full and refined between 50 and 60% for the three compounds. Thus, the two peaks of remaining electron density were treated as counterpositions of Na7 and Na8, and the corresponding atoms Na71 and Na81, respectively, were refined to add up to full occupancy. The final fractions of Na7/Na8 were 51/53, 68/45, and 68/63% for compounds **1–3**, respectively. Details of the data collections and structure refinements are given in Table 1, while important distances and angles are listed in Table 2.

Magnetic Measurements. These were carried out on a Quantum Design MPMS SQUID magnetometer. The samples were sealed in a quartz tube between two quartz rods that fit tightly in the tube. The magnetizations of 19 mg of **2** and 15 mg of **3** were measured in the temperature range 10–250 K at fields of 3 T and 300 G. The data were corrected for the holder and for ion-core diamagnetism. The resulting molar magnetic susceptibility of **2** was temperature-independent and negative, $-(2.615-1.075) \times 10^{-4}$ emu/mol, and indicated diamagnetism. Compound **3**, on the other hand, showed paramagnetic behavior with two ferromagnetic transitions at ca. 70 and 20 K.

Resistivity Measurements. The electrical resistivities of compounds **2** and **3** (two different samples) were measured by the four-probe method (an in-line probe from Jandel) on pressed pellets (2000 psi, 0.13 mm diameter) over the temperature range 224–294 K inside a cold well of a drybox. Measured was the drop of voltage across the samples at constant currents. The resistivities of both compounds decreased at increasing temperature, a behavior consistent with semiconducting compounds (room-temperature resistivities of ca. 0.11 and 0.09 $\Omega \cdot \text{cm}$ for **2** and **3**, respectively).

Results and Discussion

The structure of the three isostructural compounds contains two isolated anions: flat pentagonal rings of Tt₅⁶⁻; single-atom anions Tt⁴⁻ (Figure 1). The distances in the rings are in the ranges 3.047(1)–3.117(1), 2.894(1)–2.948(1), and 2.864(2)–2.907(2) Å for **1–3**, respectively (Table 2), with averages of 3.078, 2.921, and 2.883 Å, respectively, for the three compounds. These distances are shorter than the corresponding single-bond distances. For example, 3.13(1) Å is the Pb–Pb distance in the infinite chains of $[\text{-(Pb}^{2-}\text{)-}]$ in BaPb⁸ and 3.067(2)–3.167(3) Å is the range of Sn–Sn distances in Ca₃₁Sn₂₀ which contains isolated linear penta-

Table 2. Important Distances (Å) and Angles (deg) in Na_3BaPb_6 , Na_3BaSn_6 , and Na_3EuSn_6

	Na_3BaPb_6	Na_3BaSn_6	Na_3EuSn_6
Tt1–Tt2	3.058(1)	2.911(1)	2.876(2)
Tt2–Tt3	3.101(1)	2.939(1)	2.894(2)
Tt3–Tt4	3.047(1)	2.894(1)	2.864(2)
Tt4–Tt5	3.071(1)	2.915(1)	2.878(2)
Tt5–Tt1	3.117(1)	2.916(1)	2.907(2)
Tt5–Tt1–Tt2	106.32(4)	106.83(5)	107.35(7)
Tt1–Tt2–Tt3	108.93(4)	108.74(5)	108.37(7)
Tt2–Tt3–Tt4	108.06(4)	107.73(5)	107.91(7)
Tt3–Tt4–Tt5	107.70(4)	108.28(5)	108.32(7)
Tt4–Tt5–Tt1	108.98(4)	108.42(5)	108.05(7)
Ae/Re–Tt1 × 2	3.799(1)	3.698(1)	3.617(1)
Ae/Re–Tt2 × 2	3.672(1)	3.596(1)	3.517(1)
Ae/Re–Tt3 × 2	3.678(1)	3.603(1)	3.516(1)
Ae/Re–Tt4 × 2	3.778(1)	3.675(1)	3.599(1)
Ae/Re–Tt5 × 2	3.810(1)	3.717(1)	3.655(1)
Tt1–Na1 × 2	3.308(6)	3.312(1)	3.252(6)
Tt1–Na4 × 2	3.335(9)	3.330(4)	3.261(7)
Tt1–Na5	3.629(8)	3.642(9)	3.600(9)
Tt1–Na8	3.648(3)	3.666(9)	3.655(9)
Tt2–Na1	3.208(1)	3.192(7)	3.219(1)
Tt2–Na1 × 2	3.635(8)	3.614(5)	3.514(7)
Tt2–Na5 × 2	3.386(1)	3.415(6)	3.384(1)
Tt2–Na7	3.416(6)	3.378(9)	3.386(1)
Tt3–Na2	3.212(1)	3.211(8)	3.221(9)
Tt3–Na2 × 2	3.594(9)	3.592(6)	3.507(7)
Tt3–Na6 × 2	3.311(9)	3.321(6)	3.266(9)
Tt3–Na7	3.372(1)	3.332(9)	3.360(9)
Tt4–Na2 × 2	3.380(6)	3.372(5)	3.312(6)
Tt4–Na3 × 2	3.408(8)	3.392(5)	3.321(8)
Tt5–Na3	3.369(1)	3.222(8)	3.356(9)
Tt5–Na3 × 2	3.444(9)	3.450(6)	3.350(8)
Tt5–Na4 × 2	3.540(9)	3.529(7)	3.427(9)
Tt5–Na71	3.383(9)	3.262(9)	3.315(9)
Tt6–Na4	3.313(9)	3.250(8)	3.282(9)
Tt6–Na5	3.366(9)	3.318(8)	3.311(9)
Tt6–Na6	3.418(9)	3.342(9)	3.339(9)
Tt6–Na7 × 2	3.231(9)	3.214(6)	3.146(9)
Tt6–Na71 × 2	3.491(8)	3.342(9)	3.321(9)
Tt6–Na8	3.365(9)	3.375(9)	3.341(9)
Tt6–Na8 × 2	3.458(9)	3.412(9)	3.353(9)
Tt6–Na81	3.390(9)	3.306(9)	3.298(9)
Tt6–Na81	3.589(9)	3.557(9)	3.456(9)

mers, dimers, and single atoms.⁹ At the same time the distances in **1** are somewhat longer than the double-bond distance of 2.95(2) Å observed for the isolated $[\text{Pb}=\text{Pb}]^{4-}$ dimers in Li_8Pb_3 .¹⁰ The angles in the pentamers are very close to the ideal $3\pi/5 = 108^\circ$ and fall in the ranges 106.32(4)–108.98(4), 106.83(5)–108.74(5), and 107.35(7)–108.37(7)° for **1**–**3**, respectively (Table 2). Despite the small deviations from the ideal 108° , however, the rings are perfectly flat evidenced by the perfect 540° (3π) for their sums in all three compounds. Furthermore, the five atoms forming the rings are crystallographically independent and, therefore, the planarity of the rings is not imposed by symmetry requirements but is rather driven by bonding requirements. The small inequalities of the distances and angles within each ring are most likely due to different environments around the atoms.

The pentagonal rings are stacked exactly on top of each other in eclipsed fashion and form columns along the *b* axis

(8) Zurker, F.; Nesper, R.; Hoffmann, S.; Fassler, T. F. *Z. Anorg. Allg. Chem.* **2001**, *627*, 2211.

(9) Ganguli, A. K.; Guloy, A. M.; Escamilla, A.; Corbett, J. D. *Inorg. Chem.* **1993**, *32*, 4349.

(10) Zalkin, A.; Ramsey, W. J.; Templeton, D. H. *J. Phys. Chem.* **1956**, *60*, 1275.

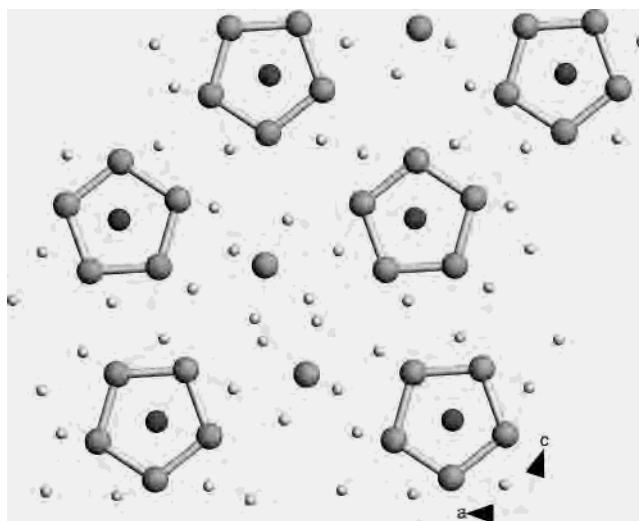


Figure 1. View of the structure of the isostructural compounds Na_3BaPb_6 , Na_3BaSn_6 , and Na_3EuSn_6 along the *b* axis of the monoclinic cell. The aromatic pentagonal rings (outlined with thick bonds) are capped from both sides by the alkaline- or rare-earth cations (darker spheres). Isolated tetrel atoms (large spheres) are found between the pentagons. The sodium cations bridge bonds in the pentagons and coordinate the isolated atoms.

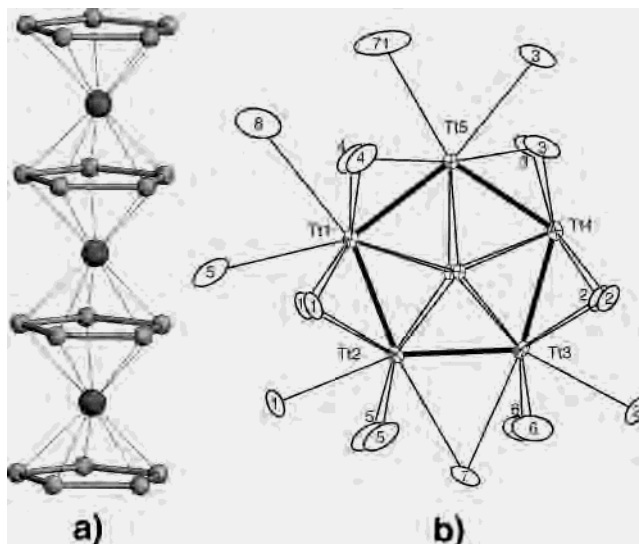


Figure 2. (a) Column of aromatic rings separated by Ae/Re cations. (b) ORTEP view of the coordination of cations around an aromatic ring of Tt_5^{6-} . (Specifically shown is Pb_5^{6-} in **1** at 40% thermal ellipsoids.)

(Figure 2a). The alkaline- or rare-earth cations are found exactly halfway between the ring planes in a ferrocene-like geometry. However, they are not exactly on the line between the centers of the rings but are rather closer to Tt2–Tt3 and farther from Tt4–Tt5–Tt1 (Figure 2b). This is most likely due to the different coordination of the tetrel atoms. Thus, while the bonds Tt3–Tt4–Tt5–Tt1–Tt2 are doubly bridged by sodium cations above and below the plane of the ring, the bond Tt2–Tt3 has one bridging atom that is within the plane (Figure 2b and Table 2). Most likely the Ae/Re cations are shifted closer to Tt2–Tt3 to provide additional bridging to this bond. The ring can be viewed as a cluster with two pentagonal faces that are capped by Ae/Re while the edges are bridged by sodium atoms. The tetrel atoms, except Tt4, are coordinated additionally by sodium exo-atoms. The latter

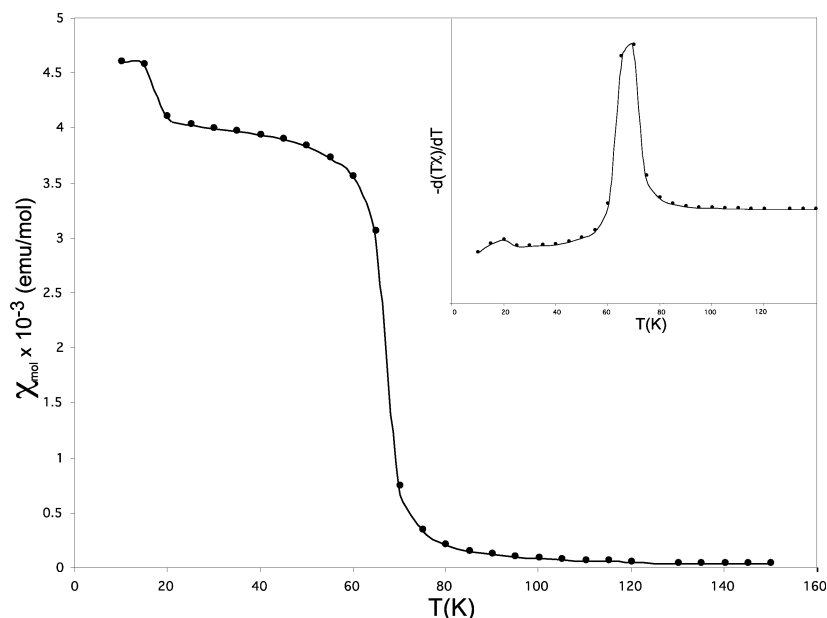


Figure 3. Molar magnetic susceptibility of Na_8EuSn_6 measured at 300 G (zero-field cooled) showing two transitions at ca. 20 and 70 K. Shown in the insert is the derivative of the magnetic moment with the two transitions clearly visible.

serve as inner bridging atoms in neighboring rings or are coordinated to the isolated Tt^{4-} anions (Figure 1). Thus, the pentagons can be considered as “interconnected” via such inner–outer sodium cations. It should be pointed out that all atoms in the structure are positioned within two planes perpendicular to the b axis with $z = 0.25$ and 0.75 .

The isolated tetrel anions Tt^{4-} are positioned within the planes of the pentagonal rings (Figure 1). They are coordinated by eight sodium cations at distances ranging from 3.231(9) to 3.589(9) Å (figure in Supporting Information). Five of these coordination sites are occupied by two cations that are each disordered among two positions, Na7/Na71 and Na8/Na81. All three compounds show exactly the same disorder although the fractions for the corresponding sites differ somewhat (see Experimental Section). The reason for the disorder is very likely the need to achieve both acceptable coordination around the tetrel anion and efficient packing with the rigid columns of rings. As it can be seen in Figure 1, the structure has some small openings between the rings and the isolated atoms, and this indicates somewhat inefficient packing. Such “holes” provide flexibility for various distribution of the cations in the structure.

The structure of the three compounds is similar to that of Li_8MgSi_6 .¹¹ The major difference between the two structures is that, surprisingly, Li and not Mg is found between the rings of Si_5^{6-} in the latter. Instead, the magnesium cations are found statistically distributed over several positions around the isolated Si^{4-} atoms. Thus, eight close positions were refined with various magnesium content, and it is not clear how accurate the distribution of the two different cations is in this structure. Nonetheless, assuming it as accurate, the different positioning of the alkali and alkaline-earth cations in the two structures may be attributed to the different sizes

of the two cations with respect to each other and the packing requirements. Thus, the somewhat smaller Mg^{2+} may be too small to separate efficiently two adjacent Si pentagons, and therefore Li^+ , is preferred there. For the three compounds reported here the situation is reversed; i.e., the alkaline- and rare-earth cations Ba^{2+} and Eu^{2+} are quite larger than Na^+ .

The stoichiometry of the new compounds can be easily rationalized within the Zintl–Klemm concept. Assuming complete electron transfer from the cations, the resulting 10 electrons are distributed between one pentagonal ring and one single atom of the tetrel, i.e., Tt_5^{6-} and Tt^{4-} , and the formula can be written as $(\text{Na}^+)_8(\text{Ae/Re}^{2+})(\text{Tt}_5^{6-})(\text{Tt}^{4-})$. This results in closed-shell formations for all the species. Tt_5^{6-} is analogous to the aromatic cyclopentadienyl anion C_5H_5^- and can be considered *arachno*-species derived from the corresponding *closo*-pentagonal bipyramid after removing the two apexes. There has been extensive recent interest in all-metal aromatic species, and numerous theoretical studies have been carried out on gas-phase molecules and some alloys.¹²

The three compounds are electronically balanced according to the results from the magnetic and four-probe conductivity measurements of compounds **2** and **3**. The black color of the crystals and their brittleness are also in agreement with this. Compound **2** showed temperature-independent and negative magnetic susceptibility indicative of diamagnetic properties. This corroborates with the observed semiconducting behavior of both **2** and **3** measured by the four-probe method. The calculated band gaps from the plots of $\ln(\rho)$ vs $1/T$ for the two compounds are ca. 0.10 and 0.12 eV in the

(11) Nesper, R.; Curda, J.; v. Schnering, H. G. *J. Solid State Chem.* **1986**, *62*, 199.

(12) (a) Xi, Li; Zhang, H.-F.; Wang, L.-S.; Kuznetsov, A. E.; Cannon, N. A.; Boldyrev, A. I. *Angew. Chem., Int. Ed.* **2001**, *40*, 1867. (b) Kuznetsov, A. E.; Zhai, H.-J.; Wang, L.-S.; Boldyrev, A. I. *Inorg. Chem.* **2001**, *41*, 6062. (c) Li, X.; Kuznetsov, A. E.; Zhang, H. F.; Boldyrev, A. I.; Wang, L. S. *Science* **2001**, *291*, 859. (d) Kuznetsov, A. E.; Corbett, J. D.; Wang, L. S.; Boldyrev, A. I. *Angew. Chem., Int. Ed.* **2001**, *40*, 3369.

region 224–294 K. The room-temperature resistivities were measured at ca. 0.11 and 0.09 $\Omega\cdot\text{cm}$ for **2** and **3**, respectively. These numbers compare well with other semiconducting intermetallics such as $\text{Ca}_{14}\text{MnAs}_{11}$ (0.18 eV, 0.10 $\Omega\cdot\text{cm}$),¹³ $\text{Sr}_{14}\text{CdSb}_{11.37}$ (0.016 eV, 0.63 $\Omega\cdot\text{cm}$),¹⁴ and $\text{Ca}_{14}\text{CdSb}_{11.43}$ (0.076 eV, 0.028 $\Omega\cdot\text{cm}$).¹⁴

According to the magnetic measurements and as expected, compound **3** is paramagnetic at higher temperatures (μ_{eff} of ca. 7.1 μ_{B}). At low temperatures it undergoes magnetic transitions at ca. 70 and 20 K (Figure 3). This is somewhat unexpected because the Eu(II) centers are quite far apart (5.220 Å) and should not be able to interact directly. Furthermore, the sample showed semiconducting properties at higher temperatures and, unless it undergoes transition to metallic state at lower temperatures, there should be no delocalized electrons that might provide the means for “magnetic communication” between the localized spins. Thus, it is possible that the π -systems of the rings provide the communication between the magnetic centers. Another peculiar magnetic behavior of this compound is the lack of hysteresis below the transition at 70 K (the measurements were done at 30 K) and the completely overlapping magnetizations measured at field-cooled and zero-field-cooled conditions. Finally, the effective magnetic moment above 70 K is somewhat lower than the spin-only 7.94 μ_{B} expected for seven unpaired electrons as in Eu(II). Measure-

ments on different samples from different reactions provided numbers between 5.8 and 7.1 μ_{B} . This is most likely due to dilution by either small amounts of nonmagnetic impurities or by partial decomposition of the sample during its preparation and transfer into the holder. Neutron diffraction studies at low temperatures and magnetic measurements at high temperatures are currently under way.

Conclusions

The anions Sn_5^{6-} and Pb_5^{6-} are the first aromatic species of such heavy metals. Together with Si_5^{6-} they are analogues of the cyclopentadienyl anion. Other ternary compounds with somewhat poorly resolved structures (at this stage) seem to contain also pentagonal rings of tin as well as germanium.

Acknowledgment. We thank John Greedan (McMaster University) for the help with interpretation of the results from the magnetic measurements and for carrying out further neutron diffraction and magnetic studies and the National Science Foundation (Grant CHE-0098004) and the Petroleum Research Fund, administered by the American Chemical Society (Grant 37301-AC5,3), for the financial support of this research.

Supporting Information Available: A view of the coordination around the isolated tetrel atoms, a plot of the temperature dependence of the molar magnetic susceptibility of compound **2**, and an X-ray crystallographic file in CIF format. This material is available free of charge via the Internet at <http://pubs.acs.org>.

IC0491837

(13) Rehr, A.; Kuromoto, T. Y.; Kauzlarich, S. M.; Castillo, J. D.; Webb, D. J. *Chem. Mater.* **1994**, *6*, 93.

(14) Young, D. M.; Torardi, C. C.; Olmstead, M. M.; Kauzlarich, S. M. *Chem. Mater.* **1995**, *7*, 93.